RERTR 2010 — 32nd INTERNATIONAL MEETING ON
REDUCED ENRICHMENT FOR RESEARCH AND TEST REACTORS

October 10-14, 2010
SANA Lisboa Hotel
Lisbon, Portugal

IMPACT OF PHOTONEUTRONS ON TRANSIENTS FOR THE MURR AND MITR HEU AND LEU CORES

B. Dionne and N. Hanan
Research and Test Reactor Conversion Department
Nuclear Engineering Division
Argonne National Laboratory, Argonne, IL 60439-4815 - USA

ABSTRACT

The University of Missouri Research Reactor (MURR) and the Massachusetts Institute of Technology Reactor (MITR) have reflectors composed of beryllium and heavy water, respectively. Both these materials produce neutrons through a (gamma, n) process which increase the effective delayed neutron fraction of these cores. To study the impact of those photo-neutrons on the neutronics transients, their contribution will be calculated for their HEU and proposed LEU cores. Then, using MCNP5 and ENDF/B-VII cross sections, the contribution to the delayed neutron faction from the reflector will be evaluated. Considering the resulting new delayed neutron fraction and group structure appropriate for either beryllium or heavy-water, PARET/ANL will be used to study both positive and negative reactivity insertion transients.

1. Introduction

The safety analyses for the conversion of reactor cores from highly-enriched (HEU) to low-enriched (LEU) uranium have so far relied on computational results to estimate the point-kinetic parameters necessary to perform the required transient analyses. These kinetic parameters are the i) prompt neutron generation lifetime, ii) reactivity feedback coefficients, and iii) effective delayed neutron fraction (β_{eff}).

For reactors reflected by D_2O (MITR-II) or Be (MURR), gamma rays leaking from the core region interact with the reflector material through (γ, n) reactions and produce photo-neutrons that contribute to the overall neutron balance of the system. These are threshold reactions such that gamma rays need to have energies larger than about 2.2 MeV and 1.6 MeV to create photo-neutrons in the D_2O and Be reflectors, respectively [1].

The impact of those photo-neutrons on transients following the conversion was raised as a Therefore, this work focuses on evaluating the effect of the photo-neutrons on β_{eff} and consequently, on transients.

In the last decade or so, because of the increase in computational resources, transport calculations (MCNP5 [2]) and a perturbation-independent methodology [3] have been used in the GTRI program to evaluate β_{eff}. More recently, the use of clusters of multi-cores machines and the parallel computation capabilities of the MCNP5 code allows taking into account neutrons generated from gamma rays interactions in the reflector in the calculation the β_{eff}. However, as it will be shown, these calculations remain outside the domain of routine application for these two reactors.

In this work, β_{eff} calculations are performed for the MITR-II and MURR cores loaded with either HEU or LEU fresh fuel elements. The delayed neutron fractions are used in PARET/ANL models [4] to simulate a series of typical transients of interest in order to illustrate their impact.

This paper is organized as follows. Section 2 briefly introduces the MITR-II and MURR reactor cores. Section 3 presents a description of the methodology. Section 4 presents the reactor transients considered in this work. Section 5 presents results and analyses while, finally, concluding remarks are presented in Section 6.

2. MITR and MURR reactors

The Massachusetts Institute of Technology Reactor (MITR-II) core is light-water cooled and moderated. It contains twenty-seven fuel positions in three radial rings with at least three positions filled with either an in-core experiment or a solid aluminum dummy element used to reduce power peaking. The fuel elements are composed of parallel fuel plates inserted diagonally between side plates and form a rhomboid-shaped element. The MITR-II hexagonal core is surrounded by boron-impregnated stainless steel control blades and by heavy-water as well as graphite reflectors.

The MITR-II current HEU and proposed LEU fuel elements have, respectively, fifteen and eighteen fuel plates. In both fuel designs, the plates are composed of a fuel meat clad by aluminum. The HEU fuel meat (30 mils thick) is composed of 93% enriched UAl_x-Al dispersion fuel (1.59 $g^{235}U/cm^3$) while the proposed LEU fuel meat (20 mils thick) is composed of 19.75% enriched U-10Mo monolithic alloy fuel (3.03 $g^{235}U/cm^3$) [5].

The Missouri University Research Reactor (MURR) is a tank-type light-water cooled and moderated reactor with eight assemblies consisting of curved fuel plates swaged between side plates to form a wedge-like structure. These fuel assemblies, located between an inner and outer pressure vessel, are arranged such that a water-filled central flux trap is formed. The outer pressure vessel is surrounded by curved B_4C-Al control blades and by beryllium as well as graphite reflectors.

Both MURR HEU and proposed LEU fuel elements have twenty-four curved fuel plates composed of a fuel meat clad by aluminum. The HEU fuel meat (20 mils thick) is composed of 93% enriched UAl_x-Al dispersion fuel (1.53 $g^{235}U/cm^3$) while the proposed LEU fuel meat (9-17 mils thick) is composed of 19.75% enriched U-10Mo monolithic alloy fuel (3.03 $g^{235}U/cm^3$) [6].

Fig. 1 shows sections of the MITR-II and MURR cores at reactor mid-plane.

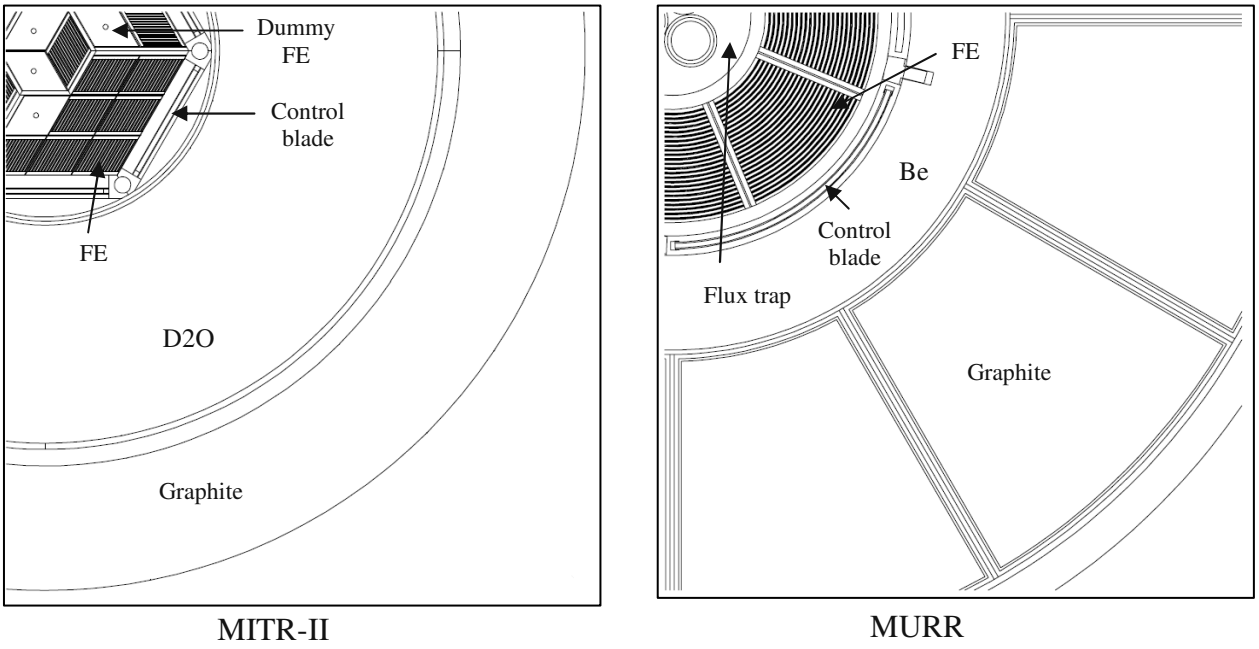

Figure 1 Section of the MITR-II and MURR reactor cores at mid-plane.

3. Methodology

Considering that the photo-neutrons are not expected to contribute significantly to either the prompt generation lifetime or the reactivity feedback coefficients; this work focuses on their impact on the β_{eff}.

3.1 Delayed neutron fraction components

For this work, the total effective delayed neutron fraction (β_{eff}^{total}) is written as the sum of three components according to the origin of the delayed neutrons as shown in Eq. (1).

$$\beta_{eff}^{total} = \beta_{eff}^{FP} + \beta_{eff}^{(\gamma,n)_p} + \beta_{eff}^{(\gamma,n)_d} \quad (1)$$

The first component, β_{eff}^{FP} , is the fraction of the effective delayed neutrons created by the fission products themselves. The second component, $\beta_{eff}^{(\gamma,n)_p}$, is the fraction of the effective delayed neutrons created through the interaction of prompt gammas with the reflector. Finally, the third

component, $\beta_{eff}^{(\gamma,n)_d}$, is the fraction of the effective delayed neutrons created through the interaction of delayed gammas with the reflector.

3.2 Perturbation-independent methodology using MCNP5

The contribution of the delayed neutrons created by the fission products is evaluated by performing an MCNP5 calculation (MODE N) with and without delayed neutrons (using the TOTNU card) and, ignoring the contribution of the photo-neutrons. β_{eff}^{FP} is then estimated using Eq. (2).

$$\beta_{eff}^{FP} = \frac{k_{eff,tot}^{FP} - k_{eff,prompt}}{k_{eff,tot}^{FP}} \tag{2}$$

The gamma rays producing photo-neutrons can be categorized as either prompt fission gammas, delayed fission gammas, prompt capture gammas and delayed capture gammas.

In this work, the photon-neutrons generated by the prompt fission and capture gammas are modeled by performing an MCNP5 coupled neutron-photon calculation (MODE NP) using the MPN cards to model (γ, n) reactions for the reflector materials only. Ignoring the contribution from the delayed gammas, Eq. (1) can be rewritten to calculate $\beta_{eff}^{(\gamma,n)_p}$ as shown in Eq. (2).

$$\beta_{eff}^{(\gamma,n)_p} = \beta_{eff}^{total} - \beta_{eff}^{FP} = \frac{k_{eff,tot}^{FP+(\gamma,n)} - k_{eff,prompt}}{k_{eff,tot}^{FP+(\gamma,n)}} - \frac{k_{eff,tot}^{FP} - k_{eff,prompt}}{k_{eff,tot}^{FP}} . \tag{3}$$

Note that all MCNP5 calculations presented in this paper were performed with ENDF/B-VI cross sections.

Since MCNP5 does not simulate delayed particles[1], the impact of the additional term $\beta_{eff}^{(\gamma,n)_d}$ is analyzed by a parametric study. The delayed gammas spectrum is slightly softer than the prompt gamma spectrum since the intensity of the high-energy gammas decays more rapidly [7]. The total energy produced per fission is slightly smaller [8] for the delayed gammas, i.e., 6.6 MeV/fission from prompt gammas and 5.6 MeV/fission for delayed gammas. For both those reasons, using the calculated value of $\beta_{eff}^{(\gamma,n)_p}$ to represent the contribution to the delayed neutrons from (γ, n) reactions of fission delayed gamma should be bounding. Since the estimation of the number and energies of beta-delayed gammas resulting from neutron capture is difficult, it will be assumed that the photo-neutrons resulting from their interaction in the reflector materials is also bounded by $\beta_{eff}^{(\gamma,n)_p}$. Therefore, the upper limit of $\beta_{eff}^{(\gamma,n)_d}$ used in this work is represented by,

[1] MCNPX v2.6 [9] and possibly the release of MCNP6 [10] allows (or will allow) for the simulation of delayed gammas

$$\beta_{eff}^{(\gamma,n)_d} = 2 \times \beta_{eff}^{(\gamma,n)_p} \quad (4)$$

In addition to β_{eff}, it is necessary to provide delayed neutron fractions and decay constants for each precursor group. To model the photo-neutrons in the point kinetics solution, additional precursor groups are added to the six traditional groups [7]. In adding precursor groups to take into account photo-neutrons (9 for D_2O and 12 for Be) [7], it is necessary to renormalize the delayed neutron fractions such that:

$$\beta_{eff}^{FP} = \sum_{i=1}^{6} \beta_i^{FP} \quad (5a) \qquad \beta_{eff}^{(\gamma,n)} = \sum_{j=1}^{9 or 12} \beta_i^{(\gamma,n)} \quad (5b)$$

Table 1 gives the half-life (in seconds) for each of the precursor groups considered for the HEU MITR-II and MURR cores with photo-neutron contributions produced by prompt gammas only.

Table 1 Delayed group structures for HEU core with photo-neutrons from prompt gammas only

	MITR-II		MURR	
	Fraction	Half-life (sec)	Fraction	Half-life (sec)
β_i^{FP}	0.39124	2.30	0.38929	2.30
	0.21695	22.73	0.21594	22.73
	0.19410	6.24	0.19346	6.24
	0.11396	0.61	0.11359	0.61
	0.04160	0.23	0.04129	0.23
	0.03276	55.90	0.03247	55.90
$\beta_i^{(\gamma,n)}$	0.00606	2.50	0.00710	4.51
	0.00191	41.00	0.00506	21.97
	0.00065	2.40	0.00109	55.94
	0.00031	7.70	0.00044	2.16
	0.00022	1.65	8.01E-05	392.60
	0.00019	27.00	5.24E-05	1206.08
	3.03E-05	4.40	4.60E-05	186.46
	9.59E-06	53.00	3.50E-05	3867.76
	3.82E-06	307.00	2.72E-05	6571.04
			2.11E-05	23955.17
			1.46E-05	11603.28
			1.91E-06	158619.80

It should be noted that the delayed neutron fractions used in the analyses are renormalized properly for each reactor and each case (HEU, LEU, photon-neutrons only from prompt gammas, photo-neutrons from prompt and delayed gammas) in order to respect Eqs. (5a) and (5b).

3.3 PARET/ANL models

The impact of the photo-neutrons on the transient behavior of both MITR-II and MURR cores is studied using PARET/ANL for a series of transients. PARET/ANL is a transient one-dimensional single-phase hydrodynamic code linked with a point kinetics solver which takes into

account fuel temperature, coolant temperature, coolant void and thermal expansion feedbacks. A simplified vapor generation model is used to evaluate void reactivity feedback and obtain an estimation of the two-phase flow thermal-hydraulics solution.

To be consistent with typical practices for research reactor safety analyses, a two-channel model was developed for each core. An average channel representing most of the core is defined to model the reactor response to a given transient while a hot channel is defined to provide information about the most limiting location. A one second "null" transient is simulated before each transient in order to stabilize the steady-state solution. Note that to clearly illustrate the impact of the photo-neutrons on the neutronics power during the transients, no decay power from prior irradiation is modeled unless specified otherwise. Table 2 provides values for the main parameters used in the PARET/ANL models of the MITR-II and MURR cores.

Table 2 Generic parameters considered in PARET/ANL models for MITR-II and MURR

	MITR-II		MURR	
	HEU	LEU	HEU	LEU
Core power (MW)	5	6	10	12
Inlet temperature (°C)	44		48.9	
Inlet pressure (Pa)	135000		413685	
Mass flux (kg/m^2-s)	3421	3093	7221	6382
Lifetime (μs)	80	60.5	66	45
Reactivity feedback				
Void (Δk/k/%void)	4.50×10^{-3}	3.95×10^{-3}	2.18×10^{-3}	2.12×10^{-3}
Coolant temp. (Δk/k/°C)	1.58×10^{-4}	6.00×10^{-6}	6.69×10^{-5}	3.21×10^{-5}
Fuel temp. (Δk/k/°C)	6.99×10^{-7}	2.84×10^{-5}	6.99×10^{-7}	1.80×10^{-5}

4. Reactor transients of interest

This work focuses on two types of transients typically considered in safety analyses. The first set of transients is selected to study the core behavior following either a large step reactivity insertion or a slow ramp reactivity insertion. For the MITR-II and MURR, these types of transients are similar to the ejection of an experiment and the uncontrolled withdrawal of a control blade. Table 3 provides details about these two transients.

Table 3 Reactivity insertion transients considered

Step	0.006 Δk in 1 ms
Slow ramp	0.0025 Δk / min from 1% to 125% of full power

A second set of transients studies the core behavior following a reactor scram from full power. For MITR-II and MURR, this second type of transient is selected to emulate the power behavior following a scram due to a loss-of-flow event. Since the residual power near the establishment of natural circulation (minimal flow) is the main physical parameters determining clad temperatures, the impact of the photo-neutrons on the residual power is of interest. For this work, times between 10 and 60 seconds after the scram are considered.

5. Results and Analyses

5.1 Delayed neutron fractions

Using the methodology described in Section 3, β_{eff}^{FP} and $\beta_{eff}^{(\gamma,n)_p}$ are calculated for the MITR-II and MURR cores fueled with either HEU and LEU elements. Table 4 gives the various delayed neutron fractions obtained.

Table 4 Delayed neutron fraction for fresh MITR and MURR cores

	β_{eff}^{FP}		$\beta_{eff}^{(\gamma,n)_p}$	
	HEU[2]	LEU	HEU	LEU
MITR-II	0.007969 (0.08%)	0.007925 (0.8%)	0.000075 (12%)	0.000050 (19%)
MURR	0.007979 (0.10%)	0.007931 (0.07%)	0.000113 (10%)	0.000064 (11%)

It can be observed that $\beta_{eff}^{(\gamma,n)_p}$ is at most about 1.5% of the delayed neutrons from fission products. Based on Eqs (1) and (4), it can be expected that the total contributions of photo-neutrons should be at most 4.5% for the MITR-II and MURR cores.

Comparing the $\beta_{eff}^{(\gamma,n)_p}$, it can be seen that the photo-neutron contribution is larger for MURR. This could be explained by: i) the energy threshold is lower is beryllium resulting in a larger of number of gammas producing photo-neutrons, and ii) a larger leakage of gammas from the MURR fueled region into the reflector. A significant decrease in $\beta_{eff}^{(\gamma,n)_p}$ for LEU cores can also be observed. This could be explained by the fact that LEU monolithic fuel has a very high density resulting in a significant reduction in the gamma leakage from the core.

The critical eigenvalues (k_{eff}) were obtained with a 1-σ statistical uncertainty of about 0.001% but because of the error propagations associated with Eqs. (2) and (3) and the small values of $\beta_{eff}^{(\gamma,n)_p}$, the statistical error on the delayed neutron fractions are much larger (see Table 4). To reach a statistical uncertainty of 0.001% on the k_{eff}, each calculation required about 35 days and 50 days on 16 Xeon/3GHz processors for the MITR-II and MURR models, respectively.

5.2 Impact of photon-neutrons on positive reactivity insertion transients

Fig. 2 shows the power as a function of time following the large step reactivity insertion described in Table 3 for the MITR-II and MURR HEU cores.

[2] The 1-σ statistical uncertainty is given between parentheses.

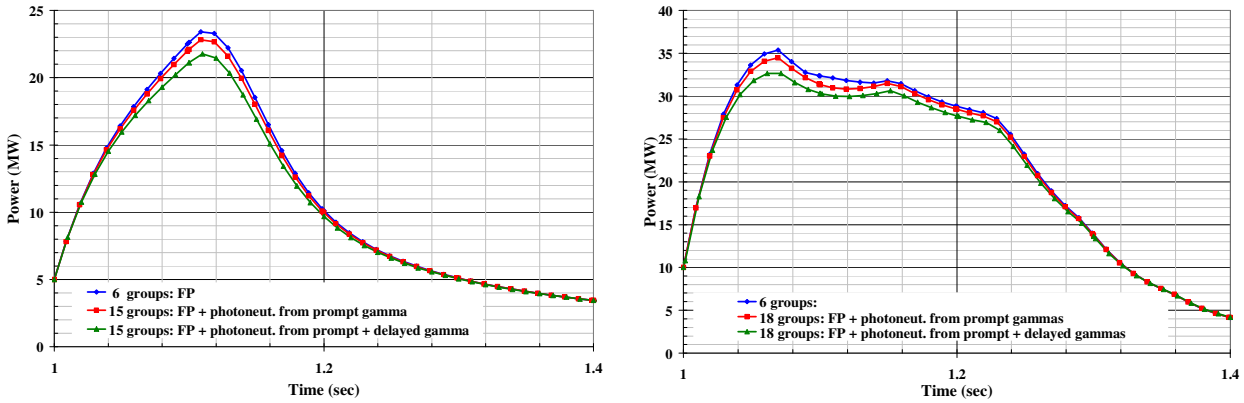

MITR-II MURR

Figure 2 HEU core power following step reactivity insertion in MITR-II and MURR cores

As expected, it can be seen that for cases where the contribution of the photo-neutrons is taken into account, the maximum power reached during the transient is smaller. This can be explained by examining the prompt factor (*PF*) (see Eq. (6)) as way to compare qualitatively two large "step" reactivity insertions. A larger *PF* indicates that a larger power will be reached at any given time during the transient.

$$PF = \frac{\beta_{eff}^{total}}{\beta_{eff}^{total} - \rho} = \frac{1}{1 - \rho / \beta_{eff}^{total}}, \tag{6}$$

where β_{eff}^{total} is the total delayed neutron fraction and ρ is the reactivity inserted.

Consequently, using Eq. (6), it can be seen that when the contribution of photo-neutrons is taken into account ($\beta_{eff}^{total} > \beta_{eff}^{FP}$), a given positive reactivity insertion results in a smaller *PF* and therefore a smaller expected power increase.

In order to compare the impact of the photo-neutrons for the HEU and LEU cores, Table 5 gives the peak power reached during the transient for the MITR-II and MURR cores.

Table 5 Peak power following step reactivity insertion for MITR-II and MURR cores

	Peak power (MW)			
	Using β_{eff}^{FP}		Using $\beta_{eff}^{FP} + \beta_{eff}^{(\gamma,n)_p}$	
	HEU	LEU	HEU	LEU
MITR-II	23.4	28.8	22.8	28.2
MURR	35.4	38.1	34.5	37.7

From Table 5, it can be seen that the difference in peak power between HEU and LEU is consistent with and without the contribution of photo-neutrons. Therefore, the change in the impact of the photo-neutrons on transients following the conversion does not appear to be a concern for step insertions.

For completeness, a small ramp reactivity insertion is also studied. Fig. 3 shows the power as a function of time following the small ramp reactivity insertion described in Table 3 for the MITR-II and MURR cores.

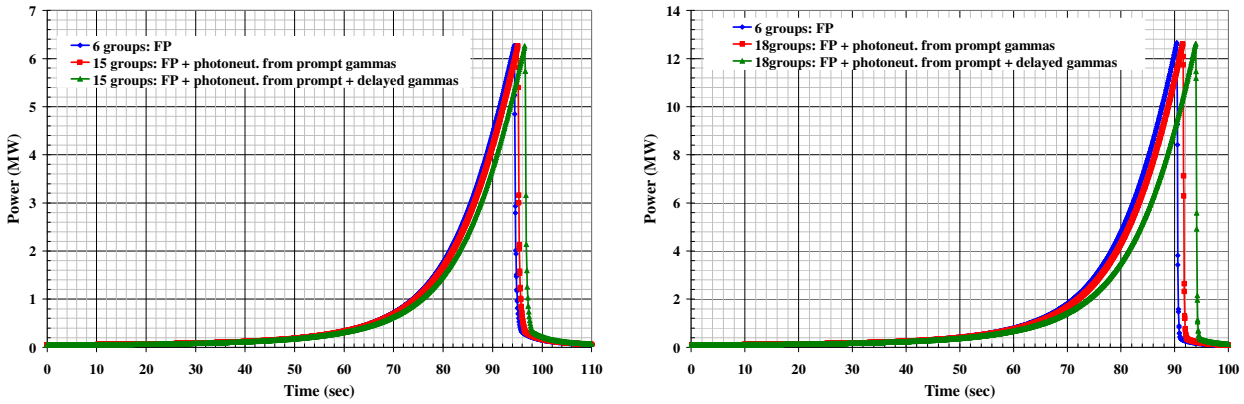

MITR-II MURR

Figure 3 HEU core power following reactivity ramp insertion for MITR-II and MURR cores

In Fig. 3, the maximum powers reached is essentially the same for all cases since the delay between the overpower trip and the actuation of the control blades do not affect the peak power due to the small and slow reactivity insertion. Therefore, the maximum powers observed in Fig. 3 are the overpower trip setting. However, the effect of the contribution of the photo-neutrons can be seen in the timing of the trip. For cases with photo-neutrons, the overpower trip is reached a few second later since, as above, the magnitude of the transient is smaller. This small change in timing does not affect any safety related parameters such as peak clad temperature.

In order to compare the impact of the photo-neutrons for the HEU and LEU cores, Table 6 gives the peak power reached during the transient for the MITR-II and MURR cores.

Table 6 Peak clad temperature following a slow reactivity ramp insertion for MITR-II and MURR cores

	Clad temperature (°C)			
	Using β_{eff}^{FP}		Using $\beta_{eff}^{FP} + \beta_{eff}^{(\gamma,n)_p}$	
	HEU	LEU	HEU	LEU
MITR-II	91.6	99.5	91.6	99.5
MURR	114.2	120.3	114.0	120.3

From Table 6, it can be seen that the difference in the peak clad temperature between HEU and LEU is consistent with and without the contribution of photo-neutrons. Therefore, the change in the impact of the photo-neutrons on transients following the conversion does not appear to be a concern for slow ramps.

5.3 Impact of photon-neutrons on negative reactivity insertion transients

Fig. 4 shows the residual neutron power as a function time following a reactor scram from full power.

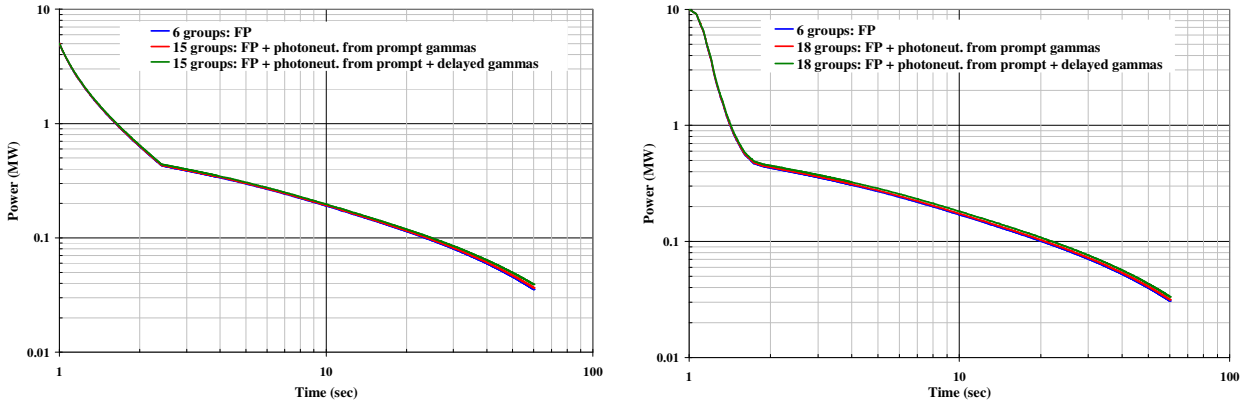

MITR-II MURR

Figure 4 HEU core power following a scram for the MITR-II and MURR core

Fig. 4 shows that, as expected, the residual neutron power remains higher when the photo-neutrons contribution is taken into account. This can be again explained using Eq. (6) which shows that, for a given negative reactive, the *PF* is larger when the contribution of the photo-neutrons is included.

In order to better quantify the change in the residual neutron power due to the contribution of the photo-neutrons, the percent differences in residual neutron power obtained with and without the contributions of photo-neutrons are given in Table 7.

Table 7 Differences in residual neutron power, after scram, with and without the photo-neutron contribution for the MITR-II and MURR cores

Time from scram (sec)	*Power obtained with* β_{eff}^{total} */ Power obtained with* $\beta_{eff}^{FP} - 1$ (%)			
	MITR-II		MURR	
	$\beta_{eff}^{total} = \beta_{eff}^{FP} + \beta_{eff}^{(\gamma,n)_p}$	$\beta_{eff}^{total} = \beta_{eff}^{FP} + 3x\beta_{eff}^{(\gamma,n)_p}$	$\beta_{eff}^{total} = \beta_{eff}^{FP} + \beta_{eff}^{(\gamma,n)_p}$	$\beta_{eff}^{total} = \beta_{eff}^{FP} + 3x\beta_{eff}^{(\gamma,n)_p}$
0.1	0.35%	1.03%	0.35%	1.03%
1.5	1.02%	3.00%	1.44%	4.31%
10	1.23%	3.82%	2.36%	7.08%
30	2.07%	6.24%	2.64%	7.92%
59	3.61%	10.78%	3.05%	9.18%

From Table 7, it can be seen that the change in residual neutron power due to the contribution of the photo-neutrons is not negligible. However, these results were obtained without taking into account the decay power from irradiation prior to the scram. It was therefore assumed that the reactors were operated continuously at full power for 45 days and 6.5 days, for the MITR-II and MURR cores respectively. Table 8 gives the percent differences in total residual power (neutron and decay power) obtained with and without the photo-neutrons contribution.

Table 8 Differences in total power, after scram, with and without the photo-neutron contribution for the MITR-II and MURR cores

Time from scram (sec)	*Power obtained with* β_{eff}^{total} */ Power obtained with* $\beta_{eff}^{FP} - 1$ (%)			
	MITR-II		MURR	
	$\beta_{eff}^{total} = \beta_{eff}^{FP} + \beta_{eff}^{(\gamma,n)_p}$	$\beta_{eff}^{total} = \beta_{eff}^{FP} + 3x\beta_{eff}^{(\gamma,n)_p}$	$\beta_{eff}^{total} = \beta_{eff}^{FP} + \beta_{eff}^{(\gamma,n)_p}$	$\beta_{eff}^{total} = \beta_{eff}^{FP} + 3x\beta_{eff}^{(\gamma,n)_p}$
0.1	0.32%	0.93%	0.32%	0.94%
1.5	0.58%	1.72%	0.77%	2.3%
10	0.50%	1.58%	0.57%	1.70%
30	0.55%	1.67%	0.37%	1.12%
59	0.57%	1.72%	0.24%	0.73%

Since the decay power is the main component of the total power after scram, it is obvious from Table 8 that the impact of including the photo-neutron contribution is significantly reduced. Considering the magnitude of the uncertainties generally involved in modeling loss-of-flow accidents, the contribution of the photo-neutrons to the total power after scram could be neglected for the MITR-II and MURR cores. Moreover, the differences in total power at 30 seconds after scram between HEU and LEU with and without the photo-neutron contribution are consistent as shown in Table 9.

Table 9 Total power 30 seconds after scram from full power for MITR-II and MURR cores

	Total power 30 seconds after scram (MW)			
	Using β_{eff}^{FP}		Using $\beta_{eff}^{FP} + \beta_{eff}^{(\gamma,n)_p}$	
	HEU	LEU	HEU	LEU
MITR-II	0.277	0.321	0.278	0.323
MURR	0.455	0.556	0.456	0.558

6. Summary and Conclusions

During the feasibility stage of the MITR-II and MURR conversion analyses, concerns were raised about the lack of modeling of the photo-neutrons produced from the gamma ray interactions in the D2O and Be reflectors when determining the delayed neutron fractions and modeling transients. The work presented in this paper focused on addressing the impact of the photo-neutrons on these two aspects using MCNP5 and PARET/ANL.

It was shown that for MITR-II and MURR, the photo-neutrons contribution to the total delayed neutron fraction is at least 20 times smaller than the contribution from the fission products. Such a small contribution is difficult to calculate precisely using Monte Carlo transport and a perturbation-independent methodology. Despite the use of significant computational resources, month-long calculations on a Linux cluster were required to reduce the statistical uncertainties.

It was also shown that, for various types of transients, ignoring the photo-neutrons is either conservative or results in negligible under-predictions in power. The bias associated with neglecting the photo-neutrons is well within the uncertainties associated with the methodologies used to evaluate the safety impact of these transients. Recent work [11] performed to evaluate the

accuracy of β_{eff} predictions using ENDF/B-VI showed discrepancies between experiments and calculations of the order of 5%. Moreover, it showed that the ratio β_{eff} / Λ (which control the behavior of the transients) can have a discrepancy with measurements of up to 14%. Therefore, parametric studies evaluating the impact of this uncertainty cover well the impact of the photo-neutrons on β_{eff}.

Finally, it was shown that the comparative studies between HEU and LEU neglecting the photo-neutrons contribution predict changes completely consistent with predictions taking into account the photo-neutrons. Therefore, neglecting the photo-neutrons has no impact of the conclusions of the MITR-II and MURR feasibility studies.

7. Acknowledgements

The authors would like to acknowledge the contributions of T. Newton (MITR) and K. Kittikad (MURR) for providing the original PARET/ANL base models as well as their patient answers to our questions.

8. References

[1] Wattenberg, A., "Photo-Neutron Sources and the Energy of the Photo-Neutrons," Physical Review, Volume 79, Number 8, pp. 497-507, April 1947.

[2] X-5 Monte Carlo Team, "MCNP-A General Monte Carlo N-Particle Transport Code, Version 5 Volumes I, II and III," LA-UR-03-1987/LA-CP-03-0245/LA-CP-03-0284, Los Alamos National Laboratory, 2003.

[3] Bretscher, M. M. ,"Perturbation-Independent Methods for Calculating Research Reactor Kinetic Parameters," ANL/RERTR/TM-30, Argonne National Laboratory, Argonne, Illinois, December 1997.

[4] Woodruff, W. L. and Smith, R. S., "A Users Guide for the ANL Version of the PARET Code, PARET/ANL (2001 Rev.)," ANL/RERTR/TM-16, Mar. 2001.

[5] Newton, T. H., et al., "Completion of Feasibility Studies on Using LEU Fuel in MIT Reactor," 31th RERTR 2009 International Meeting on Reduced Enrichment for Research and Test Reactors, Beijing, China, November 1-5, 2009.

[6.] McKibben, J., et al., "Summary of the University of Missouri Research Reactor HEU to LEU Conversion Feasibility Study," 31th RERTR 2009 International Meeting on Reduced Enrichment for Research and Test Reactors, Beijing, China, November 1-5, 2009.

[7] "Reactor Physics Constants," ANL-5800, Argonne National Laboratory, July 1963.

[8] Interpreted ENDF datafile, URL: http://www.nndc.bnl.gov/exfor/servlet/E4sGetIntSection?SectID=13084&req=91389

[9] Joe Durkee et al., "Delayed-gamma signature calculation for neutron-induced fission and activation using MCNPX. Part II: Simulations," Progress in Nuclear Energy **51** (2009) 828–836.

[10] Brown, Forest, Private communication, 2009.

[11] Santos, Adimir dos, et al., "Benchmarks on effective delayed neutron parameters and reactivity: a Brazilian IPEN/MB-01 contribution to the IRPhE project," International Conference on Reactor Physics, Nuclear Power: A Sustainable Resource Casino-Kursaal Conference Center, Interlaken, Switzerland, September 14-19, 2008.